

# MAXIMIZING INCREMENTAL INFORMATION ENTROPY FOR CONTRASTIVE LEARNING

000  
001  
002  
003  
004  
005 **Anonymous authors**  
006 Paper under double-blind review  
007  
008  
009  
010

## ABSTRACT

011 Contrastive learning has achieved remarkable success in self-supervised repres-  
012 entation learning, often guided by information-theoretic objectives such as mutual  
013 information maximization. Motivated by the limitations of static augmentations and  
014 rigid invariance constraints, we propose **IE-CL** (Incremental-Entropy Contrastive  
015 Learning), a framework that explicitly optimizes the entropy gain between aug-  
016 mented views while preserving semantic consistency. Our theoretical framework  
017 reframes the challenge by identifying the encoder as an information bottleneck and  
018 proposes a joint optimization of two components: a learnable transformation for  
019 entropy generation and an encoder regularizer for its preservation. Experiments  
020 on CIFAR-10/100, STL-10, and ImageNet demonstrate that IE-CL consistently  
021 improves performance under small-batch settings. Moreover, our core modules can  
022 be seamlessly integrated into existing frameworks. This work bridges theoretical  
023 principles and practice, offering a new perspective in contrastive learning.  
024

## 1 INTRODUCTION

025 Self-supervised contrastive learning has emerged as a cornerstone paradigm for representation learning,  
026 enabling models to extract rich semantic features without explicit labels. At its core, contrastive  
027 learning constructs a latent space where semantically similar samples converge while dissimilar  
028 ones diverge Wang & Isola (2020); Le-Khac et al. (2020). Despite rapid advances in this field, a  
029 fundamental tension persists between theoretical understanding and practical implementation. While  
030 recent works have decomposed contrastive objectives into *alignment* and *uniformity* principles Wang  
031 & Isola (2020); Zhang et al. (2023), they offer limited insight into the *dynamic information landscape*  
032 that unfolds during the learning process.  
033

034 Current contrastive frameworks such as SimCLR Chen et al. (2020a), MoCo He et al. (2020), and their  
035 variants rely heavily on static, human-engineered augmentations and large batch sampling to enforce  
036 invariance and representational diversity. These approaches impose rigid constraints on the learning  
037 dynamics: augmentations must balance semantic preservation with transformational complexity,  
038 while batch scaling faces inevitable hardware limitations. Despite substantial engineering efforts  
039 to refine augmentation strategies Chen & He (2020); Chen et al. (2021); Tian et al. (2020a), these  
040 methods fundamentally lack a principled mechanism for adaptively expanding the representational  
041 capacity of each instance while maintaining semantic coherence.  
042

043 We address this limitation by reconceptualizing contrastive learning through the lens of *incremental*  
044 *information entropy*, a novel framework that quantifies the expansion of representation space during  
045 learning. Inspired by information-theoretic objectives Hjelm et al. (2018); Bardes et al. (2022a), we  
046 focus on how additional controllable uncertainty is gained between augmented views to strengthen  
047 learning. Our key insight is that optimal contrastive learning could maximize the conditional entropy  
048 gain between positive views while preserving their mutual information. And the effectiveness of  
049 maximizing this incremental entropy is contingent on its preservation through the deep encoder,  
050 which often acts as an information bottleneck. We therefore propose a framework that jointly  
051 optimizes two synergistic components: a learnable transformation for *entropy generation* and an  
052 explicit regularization of the encoder for *entropy preservation*. This principled approach highlights  
053 the overlooked trade-off between semantic invariance and representational expressivity.

Based on this theoretical insight, we introduce **IE-CL** (Incremental-Entropy Contrastive Learning), a  
framework that explicitly optimizes for controlled entropy gain. To achieve this, we design a learnable

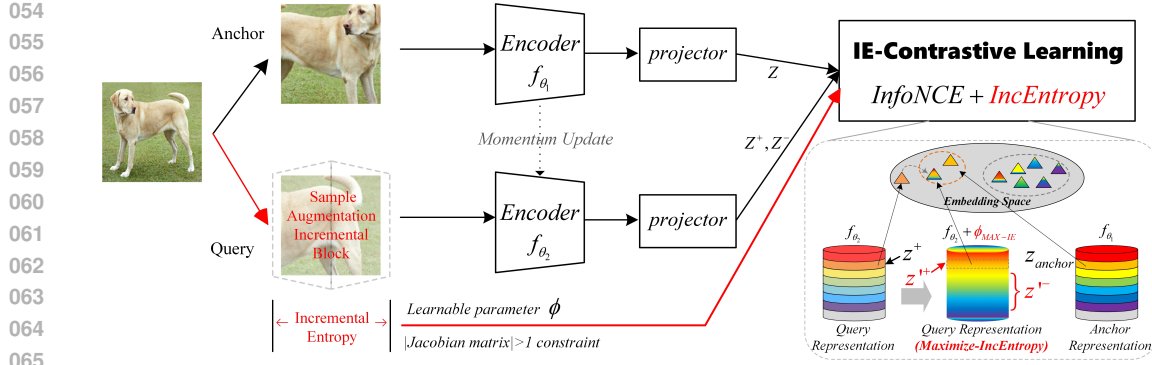


Figure 1: **Overview of the proposed IE-CL.** We define incremental entropy as the absolute change in entropy induced by classical contrastive augmentations (see Definition 3.2). To optimize the contrastive learning process, we propose the **Sample Augmentation Incremental Block (SAIB)**, a learnable module that ensures the local Jacobian determinant  $> 1$ . By incorporating sample-level incremental entropy into contrastive optimization, we establish a principled framework that improves the effectiveness of self-supervised representation learning.

nonlinear transformation module (SAIB) that adaptively expands each sample’s local representation manifold by guaranteeing a strictly positive Jacobian determinant. Crucially, to ensure this generated entropy is not lost during encoding, this module is paired with an explicit encoder regularization mechanism that encourages information preservation. These components work in concert with a Kullback-Leibler divergence constraint to balance entropic expansion against semantic consistency. IE-CL operates efficiently under small batch sizes (e.g., 256), enabling broader applicability without the hardware burden of large-batch training.

The contributions of this work can be summarised as: (1) We propose a new theoretical framework for contrastive learning that identifies the deep encoder as an information bottleneck. We posit that effective representation learning requires jointly optimizing for both **entropy generation** at the input and **entropy preservation** during encoding. (2) Based on this framework, we design a novel model, IE-CL, featuring two key components: a learnable transformation (SAIB) to generate rich input-level entropy, and an encoder regularizer (e.g., Spectral Normalisation) to ensure its faithful propagation. (3) We provide a detailed empirical analysis demonstrating IE-CL’s effectiveness, particularly in small-batch settings. We also show that our core module can enhance other self-supervised models in a plug-and-play manner.

Our work bridges the gap between information-theoretic principles and practical contrastive learning, offering a more complete theoretical understanding and algorithmic innovations that significantly advance the field of self-supervised representation learning.

## 2 RELATED WORK

**Self-supervised Paradigm** Self-supervised learning has emerged as a prominent paradigm for feature extraction without reliance on labeled dataLiu et al. (2022); Wang et al. (2023); Yang et al. (2024). A central research focus has been the development of effective encoding frameworks that facilitate rich representation learning in the absence of supervision. Notable approaches include contrastive learningChen et al. (2020b;c); Chen & He (2020); Chen et al. (2021); Caron et al. (2021); Oquab et al. (2023); Wu et al. (2023), masked autoencodersZhou et al. (2022b); Xie et al. (2022); Wei et al. (2022); Chen et al. (2022), and advances in loss function designErmolov et al. (2021); Zbontar et al. (2021); Tian et al. (2020b); Ozsoy et al. (2022); Bardes et al. (2022b). Among these, contrastive learning has become a dominant paradigm due to its ability to extract rich features through well-designed pretext tasks within a dual-encoder frameworkGarrido et al. (2022).It has frequently served as a benchmark for evaluating self-supervised learning methods. Recently, the emergence of masked pretext tasks has opened new avenues for learning representations in a label-free setting. Works such as He et al. (2021) and Bao et al. (2022) creatively adapted masking strategies from NLP to vision, enabling image reconstruction from masked tokens using spatial priors and positional embeddings. Following this, Jinghao Zhou et.alZhou et al. (2022a) further abstracted feature representations

108 in image self-supervised learning using a knowledge distillation-based masking learning strategy,  
 109 also demonstrating the effectiveness of masking strategies in dual-track self-supervised frameworks  
 110 like contrastive learning. Concurrently, the realm of non-masking pretext tasks Mo et al. (2023);  
 111 Huang et al. (2022); Oinar et al. (2023) in self-supervised learning has witnessed numerous novel  
 112 contributions. Notably, Tong et al. Tong et al. (2023) employed an extremely high number of patches  
 113 as a self-supervised signal, proposing a self-supervised learning framework requiring only one epoch.  
 114 The remarkable success of these works is largely attributable to researchers' deepening understanding  
 115 of data processing methods in self-supervised learning.

116 **Contrastive Learning Theory** The empirical success of contrastive learning has spurred extensive  
 117 theoretical investigations. Early work focused on analyzing the mathematical foundations of con-  
 118 trastive loss. Saunshi et al. Saunshi et al. (2019) were among the first to show that contrastive learning  
 119 can produce linearly separable representations under certain conditions. Wang and Isola Wang &  
 120 Isola (2020) decomposed the InfoNCE loss into two interpretable terms—alignment and uniform-  
 121 ity—where alignment promotes similarity between positive pairs and uniformity mitigates feature  
 122 collapse. This formulation offered a unified lens for understanding contrastive learning and inspired  
 123 connections to broader information-theoretic frameworks, such as mutual information maximiza-  
 124 tion Tian (2022) and noise contrastive estimation Hu et al. (2022). From a spectral graph theory  
 125 viewpoint, Chen et al. HaoChen et al. (2021) revealed that contrastive learning implicitly learns  
 126 the Laplacian of the data graph, showing equivalence to spectral clustering objectives. This was  
 127 later extended to dynamic graphs Shen et al. (2022) and connected to kernel methods Wang et al.  
 128 (2022). Tan et al. Tan et al. (2023) introduced  $\alpha$ -order mutual information to unify contrastive and  
 129 non-contrastive losses, bridging matrix-based contrastive methods (e.g., Barlow Twins Zbontar et al.  
 130 (2021), VICReg Bardes et al. (2021)) with classical dimensionality reduction techniques such as  
 131 ISOMAP. Beyond spectral perspectives, Zimmermann et al. Zimmermann et al. (2021) proposed a  
 132 probabilistic interpretation, viewing contrastive learning as reverse engineering the data generation  
 133 process under the assumption of a uniform latent prior. This aligns with the framework of noise  
 134 contrastive estimation Gutmann & Hyvärinen (2010) and sheds light on its generalization behavior.  
 135 Lee et al. Lee et al. (2021) further established a link between contrastive loss and the variational  
 136 lower bound of the data likelihood using latent variable models. As non-contrastive approaches such  
 137 as BYOL Grill et al. (2020) and Barlow Twins Zbontar et al. (2021) gained popularity, recent efforts  
 138 have focused on theoretically characterizing the distinction between contrastive and non-contrastive  
 139 paradigms Zhang et al. (2023).

### 140 3 METHOD

#### 141 3.1 INFORMATION ENTROPY IN CONTRASTIVE LEARNING

142 **Contrastive Learning Objectives** The primary goal of contrastive learning is to optimize the  
 143 similarity between positive pairs (anchor and query) while repelling negative samples, thereby  
 144 enabling effective self-supervised representation learning under the assumption of independently  
 145 and identically distributed (i.i.d.) samples within a mini-batch. For a given batch of original images  
 146  $B = \{x_i \mid i = 1, 2, \dots, N\}$ , the representation  $z_i \in Z_1$  denotes the embedding of image  $x_i$ ,  
 147 computed via the encoder  $f_{\theta_1}$ . This embedding typically originates from the anchor branch in a  
 148 dual-stream contrastive architecture. The representation  $z_i^+$  denotes the positive sample, whereas  
 149  $z_j \in Z_2$  (with  $j \neq i$ ) corresponds to negative samples derived from different instances in the batch.  
 150 These negative and positive representations are encoded by the second branch,  $f_{\theta_2}$ , and are collectively  
 151 referred to as the query set. The standard form of the objective can be expressed as:

$$152 \quad L(\mathbf{Z}_1, \mathbf{Z}_2) = -\frac{1}{N} \sum_{i=1}^N \log \frac{\exp(\text{sim}(z_i, z_i^+)/\tau)}{\sum_{j=1}^N \exp(\text{sim}(z_i, z_j)/\tau)} \quad (1)$$

155 where  $\text{sim}(z_i, z_j)$  is the similarity function, and  $\tau$  is the temperature parameter that controls the  
 156 sharpness of the probability distribution. Cosine similarity is often employed, defined as:

$$158 \quad \text{sim}(z_i, z_j) = \frac{z_i^\top z_j}{\|z_i\| \|z_j\|} \quad (2)$$

160 The optimization objective seeks to minimize the distance between each anchor and its positive  
 161 counterpart  $(z_i, z_i^+)$ , while maximizing the separation from all negative samples  $z_j \neq z_i^+$ , thereby  
 162 facilitating effective self-supervised learning.

162 **Mutual Information Theory** Mutual information provides a principled framework for analyzing  
 163 self-supervised learning objectives, as discrete probability distributions can be interpreted as samples  
 164 drawn from an underlying continuous distribution.

165 **Lemma 3.1** (Equivalence between InfoNCE minimization and mutual information maximization).  
 166 Let  $Z = f_\theta(X)$  be the embedding of input  $X$  and  $Z^+$  the corresponding positive sample. Then,  
 167 based on the Donsker–Varadhan representation, the mutual information satisfies

$$168 \min L_{\text{InfoNCE}} \iff \max I(Z; Z^+), \quad I(Z; Z^+) \geq \log N - L_{\text{InfoNCE}}.$$

170 *Proof.* The InfoNCE loss for a positive pair  $(z, z^+)$  can be written as

$$172 \quad L = -\mathbb{E}_{p(z, z^+)} \left[ \log \frac{\exp(\text{sim}(z, z^+)/\tau)}{\exp(\text{sim}(z, z^+)/\tau) + \sum_{j=1}^{N-1} \exp(\text{sim}(z, z_j^-)/\tau)} \right]. \quad (3)$$

175 Using the Donsker–Varadhan representation,

$$177 \quad I(Z; Z^+) = \sup_T \mathbb{E}_{p(z, z^+)}[T(z, z^+)] - \log \mathbb{E}_{p(z)p(z^+)}[e^{T(z, z^+)}]. \quad (4)$$

179 Choosing  $T(z, z^+) = \text{sim}(z, z^+)/\tau$  yields the lower bound

$$180 \quad I(Z; Z^+) \geq \log N - L_{\text{InfoNCE}}. \quad (5)$$

182 Thus, minimizing  $L_{\text{InfoNCE}}$  is equivalent to maximizing  $I(Z; Z^+)$ .

### 184 3.2 INCREMENTAL ENTROPY IN CONTRASTIVE LEARNING

186 It is evident that optimizing the distributions of  $Z_1$  and  $Z_2$  fundamentally depends on obtaining  
 187 effective and discriminative feature representations. From an information-theoretic standpoint—  
 188 abstracting away encoder-specific inductive biases the learning objective can be intuitively framed as  
 189 minimizing the conditional entropy  $H(Z^+|Z)$  while maximizing the marginal entropy  $H(Z^+)$ . The  
 190 incremental entropy is thus defined first from the input side.

191 **Definition 3.2** (Based on the concept of Shannon Entropy, the change in information entropy of a  
 192 given sample  $X$  after a transformation  $g$  is applied, resulting in  $X'$ , is referred to as the **Incremental  
 193 Information Entropy**).

$$194 \quad \Delta H(X) = H(X') - H(X), \quad H(X) = -\sum_i p(x_i) \log p(x_i)$$

196 The relationship between a transformation and the change in entropy can be precisely quantified. For  
 197 a linear transformation  $g$  represented by a matrix  $A$ , the incremental information entropy is given by:

$$199 \quad \Delta H(X) = H(g(X)) - H(X) = \log |\det A|$$

201 *Proof.* When the transformation  $g$  is a linear function, the probability density function of  $x$  can be  
 202 written as:

$$203 \quad p'_X(x') = p_X(A^{-1}(x' - b)) \cdot \frac{1}{|\det A|} \quad (6)$$

205 Replacing  $p'_X(x')$  with  $H(X')$ :

$$206 \quad H(X') = - \int p'_X(x') \log p'_X(x') dx' \\ 207 \\ 208 \quad = - \int p_X(A^{-1}(x' - b)) \cdot \frac{1}{|\det A|} \log \left( p_X(A^{-1}(x' - b)) \cdot \frac{1}{|\det A|} \right) dx' \quad (7)$$

210 Logarithmic term expansion:

$$212 \quad H(X') = - \int p_X(A^{-1}(x' - b)) \\ 213 \\ 214 \quad \cdot \frac{1}{|\det A|} [\log p_X(A^{-1}(x' - b)) - \log |\det A|] dx' \quad (8)$$

215 Split into two parts:

$$\begin{aligned}
216 \quad H(X') &= - \int p_X(A^{-1}(x' - b)) \\
217 \quad &\cdot \frac{1}{|\det A|} \log p_X(A^{-1}(x' - b)) dx' + \log |\det A| \\
218 \quad &\cdot \frac{1}{|\det A|} \log p_X(A^{-1}(x' - b)) dx' + \log |\det A| \\
219 \quad &\cdot \frac{1}{|\det A|} \log p_X(A^{-1}(x' - b)) dx' + \log |\det A|
\end{aligned} \tag{9}$$

220 Perform a permutation on the variable  $u = A^{-1}(x' - b)$  with  $dx' = |\det A|du$ :

$$221 \quad H(X') = - \int p_X(u) \log p_X(u) du + \log |\det A| \tag{10}$$

223 To wit:

$$224 \quad H(X') = H(X) + \log |\det A| \tag{11}$$

225 Incremental information entropy is:

$$226 \quad \Delta H(X) = H(X') - H(X) = \log |\det A| \tag{12}$$

228 This relationship makes it clear why standard augmentations have limitations. When the transformation  $g$  is a linear isometry (such as rotation, cropping, mirroring, etc.), its matrix representation  $A$  has  
229 a determinant  $|\det A| = 1$ , which leads to  $\Delta H = 0$ . In such cases, these augmentations can enrich  
230 sample diversity at the batch-level without altering the instance-level entropy.  
231

232 However, a critical challenge arises from the nature of deep encoders themselves. In information  
233 theory, the Data-Processing Inequality states that post-processing cannot increase information. For  
234 differential entropy, this implies that the entropy of a variable's representation  $Z = f(X)$  is bounded  
235 by the entropy of the original variable  $X$ . Specifically, for a deterministic function  $f$ , the change in  
236 entropy is governed by:  
237

$$H(f(X)) \leq H(X) + \mathbb{E}_{p(x)}[\log |\det J_f(x)|] \tag{13}$$

239 where  $J_f(x)$  is the Jacobian of the transformation  $f$  at  $x$ . This inequality highlights a crucial  
240 issue in representation learning: a deep encoder, acting as the function  $f$ , can potentially become  
241 an information bottleneck, diminishing the entropy of its input. Any diversity generated at the  
242 input level is not guaranteed to be preserved in the final representation space. To address this, we  
243 introduce the IE-CL framework, a holistic approach that pairs an entropy generation module with an  
244 entropy-preserving encoder. We formalize this approach in the following proposition.  
245

**Proposition 3.3** (Principle of Constrained Incremental Entropy Maximization). *Let  $X^-$  be a negative sample,  $g_\phi$  be a non-linear transformation, and  $Z'^- = f_\theta(g_\phi(X^-))$  be the final representation encoded by an encoder  $f_\theta$ . To robustly increase the representation entropy  $H(Z'^-)$ , maximizing the input-level incremental entropy  $\Delta H(X^-)$  alone is insufficient. A joint condition is required: (1) **Input Entropy Generation**: The transformation  $g_\phi$  must be optimized to maximize the incremental entropy  $\Delta H(X^-)$ . (2) **Encoder Entropy Preservation**: The encoder  $f_\theta$  must be simultaneously constrained to preserve the entropy of its input. Satisfying both conditions provides a principled path toward maximizing the diversity of negative representations for effective contrastive learning.*

253 **Theoretical Argument.** Our argument is based on the Data-Processing Inequality for differential  
254 entropy. Let  $X' = g_\phi(X^-)$  be the transformed input to the encoder. The entropy of the final  
255 representation,  $Z'^- = f_\theta(X')$ , is bounded as follows:  
256

$$H(Z'^-) = H(f_\theta(X')) \leq H(X') + \mathbb{E}_{p(x')}\log |\det J_{f_\theta}(x')| \tag{14}$$

258 This inequality reveals the core challenge. The first condition, maximizing  $\Delta H(X^-)$ , is equivalent  
259 to maximizing  $H(X')$  since  $H(X^-)$  is a constant with respect to the parameters  $\phi$  of  $g_\phi$ . However,  
260 even if  $H(X')$  is large, the second term, which depends on the Jacobian of the encoder  $f_\theta$ , can be a  
261 large negative value, effectively nullifying the gains from the first term. This occurs if the encoder  
262 acts as a strong information bottleneck, aggressively compressing its input space.  
263

Therefore, to guarantee that a large  $H(X')$  induces a correspondingly large  $H(Z'^-)$ , we introduce  
the second requirement: constraining the encoder. Specifically, by regularizing  $f_\theta$  to be entropy-  
preserving (e.g., via Lipschitz continuity constraints), we effectively bound the term  $\mathbb{E}[\log |\det J_{f_\theta}|]$ ,  
thus preventing it from becoming excessively negative. This condition ensures that the entropy  
injected by  $g_\phi$  is faithfully propagated to the final representation space.  
264

Consequently, the joint optimization of an entropy-generating transformation and an entropy-  
preserving encoder is a necessary and sufficient strategy to robustly increase the final representation  
entropy  $H(Z'^-)$ .  
265

270 3.3 MAXIMIZING INCREMENTAL INFORMATION ENTROPY  
271

272 Based on the framework established in Proposition 3.3, our goal is to co-optimize both the generation  
273 of incremental entropy and its preservation through the encoder. While encoder regularization is  
274 implemented via standard techniques such as spectral normalization, the core of our contribution  
275 lies in the design of a learnable, entropy-generating transformation  $g_\phi$ . Isometric transformations, as  
276 discussed, cannot linearly provide incremental information entropy. To address this, we propose a  
277 nonlinear transformation implemented via batch-level pixel-wise operations, explicitly designed to  
278 induce positive entropy increments in the query branch.

279 **Sample Augmentation Incremental Block (SAIB)** Our objective is to maximize mutual in-  
280 formation by minimizing the conditional entropy  $H(Z^+ | Z)$  on the query side. To inject a  
281 semantics-preserving but entropy-expansive transform into the **query branch**<sup>1</sup> we introduce the *SAIB*  
282 module, which couples ViT-style positional encoding Dosovitskiy et al. (2020) with a non-linear  
283 residual stack. The input  $X \in \mathbb{R}^{3 \times H \times W}$  is first patchified into a matrix  $P \in \mathbb{R}^{(CH/pW/p) \times (p^2)}$   
284 (as in ViT,  $C = 3$ ), where the *mini-batch* occupies the channel dimension. A sequence of  
285  $1 \times 1$  – Conv  $\rightarrow 3 \times 3$  – Conv  $\rightarrow 1 \times 1$  – Conv layers—with channel expansion ratio 2—is  
286 wrapped by two skip connections (see Appendix Figure 6). Owing to the channel-expanding residual  
287 design, the local Jacobian  $A$  of SAIB satisfies  $|\det A| > 1$  almost everywhere (Appendix C.1),  
288 guaranteeing positive incremental entropy  $\Delta H(P) > 0$ . After the non-linear block we reshape  $P'$   
289 back to the spatial layout and add a troisième skip connection  $X' = X + \text{reshape}(P')$ .

290 **KL regularisation to avoid degenerate  $g_\phi$ .** Because  $g_\phi$  acts only on the query branch, aggressive  
291 entropy expansion may lead to distributional drift. We therefore penalise the *Kullback–Leibler*  
292 *divergence*

$$294 D_{\text{KL}}(p_\phi \parallel q) = \int p_\phi(\mathbf{z}) \log \frac{p_\phi(\mathbf{z})}{q(\mathbf{z})} d\mathbf{z}, \quad (15)$$

295 where  $p_\phi(\mathbf{z}) = p(Z^- = \mathbf{z})$  is the SAIB-transformed query distribution and  $q(\mathbf{z}) = p(Z = \mathbf{z})$  is the  
296 anchor distribution. Assuming  $q$  is Gaussian with mean  $\mu$  and variance  $\sigma_0^2 I$ ,

$$299 D_{\text{KL}}(p_\phi \parallel q) = H(Z^-) + \frac{\|\mu_\phi - \mu\|^2}{2\sigma_0^2} + \frac{d}{2} \log(2\pi\sigma_0^2), \quad (16)$$

300 where  $\mu_\phi = \mathbb{E}[Z^-]$  and  $d$  is the feature dimension.

302 **Overall objective.** Our final objective function holistically integrates all components of the frame-  
303 work established in Proposition 3.3. We minimise the combined loss:

$$305 \mathcal{L}_{\text{final}} = \mathcal{L}_{\text{InfoNCE}} + \beta D_{\text{KL}}(p_\phi \parallel q) - \lambda H(Z^-) + \eta \mathcal{L}_{\text{reg\_encoder}} + \gamma R(g_\phi) \quad (17)$$

307 with  $\lambda, \beta, \eta, \gamma > 0$ . Here, the InfoNCE loss drives the primary representation learning task, while the  
308 KL-divergence term ensures that the transformations induced by SAIB maintain semantic consistency.  
309 The negative entropy term,  $-\lambda H(Z^-)$ , directly optimizes for greater diversity in the representation  
310 space, serving as the practical objective for maximizing *incremental* entropy. Crucially, the novel  
311 encoder regularizer,  $\eta \mathcal{L}_{\text{reg\_encoder}}$ , operationalizes the entropy preservation principle central to our  
312 framework, ensuring that the diversity generated by SAIB is not lost during encoding. The final  
313 term,  $\gamma R(g_\phi)$ , is an optional weight-decay penalty on the SAIB module’s parameters. This unified  
314 objective enables an end-to-end optimization of both entropy generation and preservation, yielding  
315 more robust representations.

316 4 EXPERIMENT & RESULT  
317318 4.1 EXPERIMENTAL SETUP  
319

320 **Implementation Details** We conducted upstream self-supervised learning experiments on CIFAR-  
321 10 Krizhevsky et al. (2009), CIFAR-100 Krizhevsky et al. (2009), STL-10 Coates et al. (2011), and  
322 ImageNet Deng et al. (2009), followed by downstream evaluation on the PASCAL VOC. To ensure

323 <sup>1</sup>The query branch corresponds to the lower path in Fig. 1, whose encoder parameters are  $f_{\theta_2}$ .

fair comparison, we used ResNet-based encoders across all experiments and fixed the random seed to 42 for reproducibility. For large-scale pretraining, we employed ResNet-50 as the backbone and followed the standard MoCo configuration on ImageNet for a consistent evaluation protocol. For ablation and scalability analysis, we used ResNet-18 with a batch size of 256 across CIFAR-10, CIFAR-100, STL-10, and ImageNet, enabling controlled comparisons under limited capacity settings. This phase primarily showcases the effectiveness of the proposed method under smaller batch settings across varying dataset distributions.

Table 1: The comparison of the proposed method with ResNet-50 as the backbone under different numbers of pre-training iterations. Using **BOLD** and Underline formatting to highlight the best and second results.

Method	100 ep	200 ep	400 ep	800 ep	Batch Size
SimCLR (ICML'20) Chen et al. (2020a)	66.5	68.3	69.8	71.1	4096
SwAV (NeurIPS'20) Caron et al. (2020)	66.5	69.1	70.7	71.0	4096
MoCo-v2 (CVPR'20) Chen et al. (2020c)	67.4	69.9	70.9	71.3	256
SimSiam (ICCV'21) Chen & He (2020)	68.1	<u>70.0</u>	70.8	71.7	256
NNCLR (ICCV'21) Dwibedi et al. (2021)	65.4	<u>66.1</u>	66.8	68.7	1024
All4One (ICCV'23) Estepa et al. (2023)	65.4	66.0	66.6	68.9	1024
Matrix-SSL (ICML'24) Zhang et al. (2023)	<b>69.2</b>	69.9	<u>71.1</u>	<u>71.9</u>	512
Ours	<u>68.3</u>	<b>70.9</b>	<b>71.7</b>	<b>73.2</b>	<b>256</b>

**Model Architectures** IE-CL was implemented on top of the MoCo framework, incorporating a momentum encoder and a symmetric contrastive loss as in SimCLR Chen & He (2020). A ResNet backbone with the classification head removed was used symmetrically on both anchor and query branches. The output features are 256-dimensional, obtained by global average pooling. Each branch uses a symmetric three-layer projector with an MLP-BN architecture. The hidden dimension is set to 4096, and the final projection is 512-dimensional. The anchor encoder and SAIB module are updated via backpropagation, while the query encoder is updated using momentum-based moving averages. The pseudo-code of IE-CL is shown in Appendix-Algorithm 1.

**Optimization and Hyperparameters** We trained IE-CL using AdamW with a batch size of 256, a base learning rate of 0.3, weight decay of 1e-5, and momentum of 0.9. Learning rates were scheduled via cosine annealing. The momentum coefficient  $m$  for the momentum encoder was set to 0.9. The regularization weights for our final objective (Eq. 17) were configured as  $\lambda = 0.2$  for entropy maximization,  $\beta = 0.09$  for the KL-divergence, and  $\gamma$  is 1e-4 for the SAIB weight decay. Crucially, the entropy-preserving encoder regularizer,  $\mathcal{L}_{\text{reg\_encoder}}$ , was implemented by applying Spectral Normalization to every convolutional layer of the encoder  $f_\theta$ , and its corresponding weight was set to  $\eta = 1.0$  as it is an architectural constraint rather than a loss term. For linear evaluation, we used SGD with batch sizes of 512, learning rate of 0.03, momentum of 0.9, and weight decay of 1e-5. Cosine annealing was also used for scheduling. The linear classifier was trained for 200 epochs, and we report the final epoch accuracy. All experiments were conducted on 8  $\times$  NVIDIA Tesla V100 GPUs (32GB), using PyTorch 1.13 and Python 3.8.

Table 2: Comparison of self-supervised learning methods on various datasets (left) and segmentation/detection performance on PASCAL VOC2012 (right).

(a) Comparison based on **ResNet-18** with batch size is 256.

Method	CIFAR-10	CIFAR-100	STL-10	ImageNet	(b) Results on PASCAL VOC2012 with ResNet-50 SSL pretrained.			
Pretrained	mIoU	mAP						
DeepCluster (ECCV'18) Caron et al. (2018)	84.3	50.1	79.1	41.1				
SimCLR (ICML'20) Chen et al. (2020a)	91.1	65.3	90.1	52.4				
MoCo-v2 (CVPR'20) He et al. (2020)	91.3	68.3	88.9	52.5				
BYOL (NeurIPS'20) Grill et al. (2020)	<u>91.9</u>	<u>69.2</u>	91.3	53.1				
SimSiam (ICCV'21) Chen & He (2020)	91.2	64.4	90.5	33.2				
W-MSE (ICML'21) Ermolov et al. (2021)	90.6	64.5	87.7	47.2				
MoCo-v3 (ICCV'21) Chen et al. (2021)	91.8	68.8	91.4	56.1				
S3OC (TNNLS'22) Li et al. (2022)	91.0	65.2	91.4	-				
MinEnt (PR'23) Li et al. (2023)	90.8	66.1	<u>91.5</u>	-				
Light-MoCo (ICML'23) Lin et al. (2023)	-	-	-	<u>57.9</u>				
Ours	<b>92.1</b>	<b>69.5</b>	<b>91.9</b>	<b>59.4</b>	Ours	<b>78.12</b> ( $\uparrow$ 1.21)	<b>74.41</b> ( $\uparrow$ 0.65)	

378  
379

## 4.2 MAIN RESULTS

380  
381  
382  
383  
384  
385  
386  
387  
388  
389

**Linear Evaluation** We adopt the standard linear evaluation protocol Chen et al. (2020a); Grill et al. (2020); He et al. (2021), in which the pretrained anchor encoder is frozen, and a linear classifier is trained on top. The anchor encoder, with the backbone network parameters frozen, is used for the linear evaluation process. A linear layer is appended and trained using supervised signals while keeping the backbone fixed. Training data is augmented via random horizontal flipping, random cropping to  $224 \times 224$ , and layer normalization. For evaluation, input images are resized from  $256 \times 256$  to  $224 \times 224$ . Table 1 reports Top-1 accuracy after IE-CL pretraining on ImageNet using ResNet-50 over 100, 200, 400, and 800 epochs. Table 2 shows linear probe results on other datasets using ResNet-18 (trained for 300 epochs on ImageNet and 1,000 on smaller datasets). IE-CL consistently outperforms previous baselines across all settings.

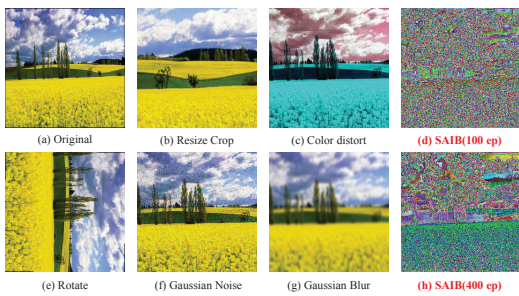
400  
401  
402  
403  
404  
405  
406

Figure 2: Illustration of the data augmentation operators studied. The non-isometric transformation operator SAIB has learnable parameters, enabling non-prior augmentation for contrastive learning. Visualizing changes from 100 epochs (d) to 400 epochs (h) shows that KL divergence effectively constrains incremental entropy, preventing collapse.

407  
408  
409  
410  
411  
412  
413

**Transfer Learning** To assess the transferability of the learned representations, we evaluate IE-CL on two downstream tasks from PASCAL VOC 2012 Everingham et al. (2010): object detection and semantic segmentation. We use Faster R-CNN Ren et al. (2016) for object detection and DeepLab-v3 Chen et al. (2018) for segmentation, both with ResNet-50 backbones pretrained via IE-CL. For segmentation, training samples are augmented with random cropping and contrast-based enhancement. Adam is used with a learning rate of  $3 \times 10^{-4}$ . For detection, the model is trained using SGD with a learning rate of  $1 \times 10^{-4}$ .

414  
415  
416  
417  
418

**Augmentation Dependency** As SAIB is implemented at the data loading stage (see Appendix Algorithm 1), it can be interpreted as a learnable augmentation layer, contrasting with traditional pretext-based augmentation schemes used in prior contrastive methods. Figure 3 presents comparative results for various augmentation strategies on ImageNet-100, under 100 epochs of pretraining and linear evaluation. Our method exhibits robust performance gains under limited augmentation.

419  
420  
421  
422  
423  
424  
425  
426  
427  
428  
429  
430

**Ablation Study** To assess the contribution of each component in IE-CL, we performed an ablation study based on a MoCo-v2 baseline with a ResNet-18 backbone on ImageNet-1k. As shown in Table 3, progressively adding the core modules in Proposition 3.3 yields consistent gains. Introducing the SAIB module for *entropy generation* produces the largest improvement, confirming the benefit of maximizing input-level incremental entropy, while the KL-divergence term for *semantic consistency* further enhances performance by mitigating distributional drift. Crucially, the final row demonstrates that incorporating our proposed *entropy preservation* mechanism via an encoder regularizer (‘Encoder Reg.’) provides an additional performance boost on top of the already strong SAIB+KL configuration. This result provides strong empirical evidence for the central tenet of our framework: that optimal performance is achieved by jointly optimizing for both entropy generation at the input and entropy preservation through the encoder. We also found that cascading multiple SAIB modules offered diminishing returns, shown in Table 4, thus we use a single module in our main configuration.

431

**Plug and Play** Table 5 demonstrates the plug-and-play ability of SAIB when integrated into other self-supervised learning frameworks on ImageNet-100, including non-contrastive methods such as



Figure 3: Ablation tests the relationship between SAIB and the previous pretext task. The image was resized to  $224 \times 224$ , and augmentation strength settings from Chen et al. (2020a) were applied, followed by two-by-two tests with SAIB placed on both sides of the contrastive learning.

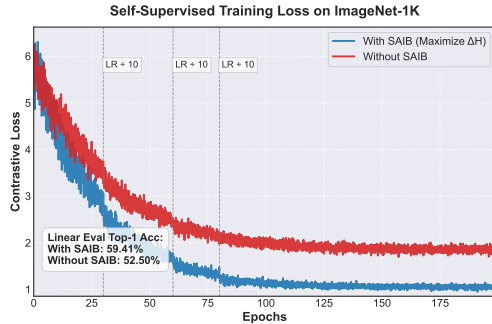
432 BYOL and SimSiam. At this point, SAIB is placed on the *Target* side, similar to its placement on the  
 433 *Anchor* side in contrastive learning. We further visualize entropy gains during training in Figure 4  
 434 and 5, showing accelerated convergence and performance improvement attributed to SAIB.  
 435

436 Table 3: Ablation study of the IE-CL components on ImageNet-1k using MoCo-v2 with a ResNet-18  
 437 backbone. We incrementally add our proposed components: the SAIB module for entropy generation,  
 438 KL regularization for semantic consistency, and an Encoder Regularizer (implemented via Spectral  
 439 Normalization) for entropy preservation.

440	Configuration	441 SAIB	442 KL Reg.	443 Encoder Reg.	444 Top-1
442	MoCo-v2 (Baseline)	✗	✗	✗	52.50
443	+ Entropy Generation	✓	✗	✗	58.80
444	+ Semantic Consistency	✓	✓	✗	59.15
445	<b>IE-CL (Full Framework)</b>	✓	✓	✓	<b>59.41</b>

446  
 447 Table 4: Ablation on the number of cascaded SAIB  
 448 modules within the full IE-CL framework. Performance  
 449 slightly degrades with more than one module,  
 450 indicating diminishing returns.

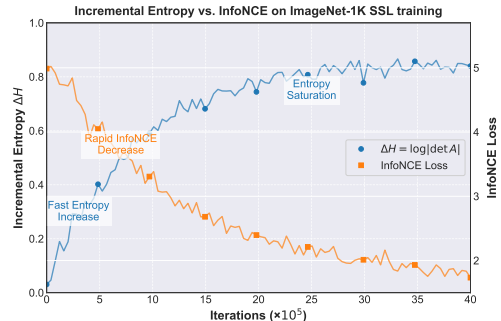
451 Configuration	452 SAIB Cascade	453 Top-1
452 IE-CL (Full Framework)	1x	<b>59.41</b>
454 IE-CL with more modules	2x	58.62
455	3x	58.71



468 Figure 4: Comparison of SSL training loss drop  
 469 curves based on the proposed maximized incremental  
 470 information entropy (SAIB) on ImageNet-1K, using  
 471 MoCo-v2 as the baseline.

472 Table 5: Based on the theory of maximizing incremental  
 473 information entropy with non-isometric trans-  
 474 formations, SAIB can be seamlessly integrated to en-  
 475 hance other self-supervised paradigms.

Method	Top1	Batch Size	Epoch
MoCo-v2	66.29	256	200
BYOL	67.95	256	200
SimCLR	63.34	256	200
SimSiam	66.25	256	200
MoCo-v2 + SAIB	67.54 ( $\uparrow 1.25$ )	256	200
BYOL + SAIB	68.76 ( $\uparrow 0.81$ )	256	200
SimCLR + SAIB	64.02 ( $\uparrow 0.68$ )	256	200
SimSiam + SAIB	66.97 ( $\uparrow 0.72$ )	256	200



5 DISCUSSION, LIMITATION, CONCLUSION AND FUTURE WORK

476 Figure 5: The variation of the incremental entropy  
 477  $\Delta H(X)$  on the Query side and InfoNCE throughout  
 478 the iterations is shown.

479 This work introduces *Sample Incremental Information Entropy* and presents a new framework, IE-CL,  
 480 to advance mutual information maximization in contrastive learning. It solves the critical challenge  
 481 of the encoder information bottleneck by jointly optimizing for *entropy generation*, via a novel  
 482 learnable transformation module (SAIB), and *entropy preservation*, via an explicit encoder regularizer.  
 483 Our approach yields consistent improvements across various datasets, though several aspects merit  
 484 further study. SAIB operates at the patch level and induces local pixel-space variations, which  
 485 preserve semantic consistency but may limit expressiveness in modeling complex structures or higher-  
 486 resolution tasks. Its reliance on convolutional priors also raises challenges for extension to vision  
 487 transformers. Nonetheless, the core principle of IE-CL, explicitly modeling and maximizing sample  
 488 entropy, provides a principled strategy for augmentation design and entropy-aware optimization,  
 489 enriching representation diversity and deepening the information-theoretic understanding of self-  
 490 supervised learning

486 ETHICS STATEMENT  
487488 This work does not involve human subjects, personally identifiable information, or sensitive medical  
489 data. All experiments are conducted on publicly available benchmark datasets (CIFAR-10/100, STL-  
490 10, ImageNet, and PASCAL VOC), which are widely adopted in the research community. We adhere  
491 strictly to the ICLR Code of Ethics and the licensing terms of the datasets used. Our proposed method,  
492 IE-CL, is intended for advancing self-supervised learning research in computer vision and does not  
493 present foreseeable risks of harmful misuse. We disclose all relevant implementation details, maintain  
494 academic integrity, and ensure that our research complies with ethical standards of reproducibility,  
495 transparency, and fairness.496  
497 REPRODUCIBILITY STATEMENT  
498499 We have made extensive efforts to ensure the reproducibility of our results. A detailed description of  
500 the proposed method, IE-CL, including the theoretical derivations (Section 3), algorithm design (SAIB  
501 module), and the overall objective function, is provided in the main text. The experimental setup,  
502 datasets, and evaluation protocols are described in Section 4, with optimization hyperparameters and  
503 implementation details explicitly listed. Additional pseudo-code and derivations are included in the  
504 Appendix. We will release the source code, training scripts, and configuration files after the paper  
505 is accepted, as supplementary materials to enable full reproducibility. Random seeds and hardware  
506 specifications are also reported to facilitate consistent replication of our experiments.507  
508 REFERENCES  
509510 Hangbo Bao, Li Dong, Songhao Piao, and Furu Wei. BEiT: BERT Pre-Training of Image Transform-  
511 ers, September 2022. URL <http://arxiv.org/abs/2106.08254>. arXiv:2106.08254  
512 [cs].  
513 Adrien Bardes, Jean Ponce, and Yann LeCun. Vicreg: Variance-invariance-covariance regularization  
514 for self-supervised learning. *arXiv preprint arXiv:2105.04906*, 2021.  
515 Adrien Bardes, Jean Ponce, and Yann LeCun. Vicreg: Variance-invariance-covariance regularization  
516 for self-supervised learning. In *International Conference on Learning Representations (ICLR)*,  
517 2022a. URL <https://arxiv.org/abs/2105.04906>.  
518 Adrien Bardes, Jean Ponce, and Yann LeCun. VICReg: Variance-Invariance-Covariance Regular-  
519 ization for Self-Supervised Learning, January 2022b. URL <http://arxiv.org/abs/2105.04906>. arXiv:2105.04906 [cs].  
520 Mathilde Caron, Piotr Bojanowski, Armand Joulin, and Matthijs Douze. Deep Clus-  
521 tering for Unsupervised Learning of Visual Features. pp. 132–149, 2018. URL  
522 [https://openaccess.thecvf.com/content\\_ECCV\\_2018/html/Mathilde\\_Caron\\_Deep\\_Clustering\\_for\\_ECCV\\_2018\\_paper.html](https://openaccess.thecvf.com/content_ECCV_2018/html/Mathilde_Caron_Deep_Clustering_for_ECCV_2018_paper.html).  
523 Mathilde Caron, Ishan Misra, Julien Mairal, Priya Goyal, Piotr Bojanowski, and Armand  
524 Joulin. Unsupervised Learning of Visual Features by Contrasting Cluster Assignments. In  
525 *Advances in Neural Information Processing Systems*, volume 33, pp. 9912–9924. Curran As-  
526 sociates, Inc., 2020. URL <https://proceedings.neurips.cc/paper/2020/hash/70feb62b69f16e0238f741fab228fec2-Abstract.html>.  
527 Mathilde Caron, Hugo Touvron, Ishan Misra, Hervé Jégou, Julien Mairal, Piotr Bojanowski, and Ar-  
528 mand Joulin. Emerging Properties in Self-Supervised Vision Transformers. pp. 9650–9660, 2021.  
529 URL [https://openaccess.thecvf.com/content\\_ICCV2021/html/Caron\\_Emerging\\_Properties\\_in\\_Self-Supervised\\_Vision\\_Transformers\\_ICCV\\_2021\\_paper.html](https://openaccess.thecvf.com/content_ICCV2021/html/Caron_Emerging_Properties_in_Self-Supervised_Vision_Transformers_ICCV_2021_paper.html).  
530 Liang-Chieh Chen, Yukun Zhu, George Papandreou, Florian Schroff, and Hartwig Adam. Encoder-  
531 decoder with atrous separable convolution for semantic image segmentation. In *Proceedings of the  
532 European conference on computer vision (ECCV)*, pp. 801–818, 2018.

540 Ting Chen, Simon Kornblith, Mohammad Norouzi, and Geoffrey Hinton. A Simple Framework for  
 541 Contrastive Learning of Visual Representations, June 2020a. URL <http://arxiv.org/abs/2002.05709>. arXiv:2002.05709 [cs, stat].  
 542

543 Ting Chen, Simon Kornblith, Kevin Swersky, Mohammad Norouzi, and Geoffrey Hinton. Big  
 544 Self-Supervised Models are Strong Semi-Supervised Learners, October 2020b. URL <http://arxiv.org/abs/2006.10029>. arXiv:2006.10029 [cs, stat].  
 545

546 Xiaokang Chen, Mingyu Ding, Xiaodi Wang, Ying Xin, Shentong Mo, Yunhao Wang, Shumin Han,  
 547 Ping Luo, Gang Zeng, and Jingdong Wang. Context Autoencoder for Self-Supervised Representa-  
 548 tion Learning, May 2022. URL <http://arxiv.org/abs/2202.03026>. arXiv:2202.03026  
 549 [cs].  
 550

551 Xinlei Chen and Kaiming He. Exploring Simple Siamese Representation Learning, November 2020.  
 552 URL <http://arxiv.org/abs/2011.10566>. arXiv:2011.10566 [cs].  
 553

554 Xinlei Chen, Haoqi Fan, Ross Girshick, and Kaiming He. Improved Baselines with Momen-  
 555 tum Contrastive Learning, March 2020c. URL <http://arxiv.org/abs/2003.04297>.  
 556 arXiv:2003.04297 [cs].  
 557

558 Xinlei Chen, Saining Xie, and Kaiming He. An Empirical Study of Training Self-Supervised  
 559 Vision Transformers, August 2021. URL <http://arxiv.org/abs/2104.02057>.  
 560 arXiv:2104.02057 [cs].  
 561

562 Adam Coates, Andrew Ng, and Honglak Lee. An analysis of single-layer networks in unsupervised  
 563 feature learning. In *Proceedings of the fourteenth international conference on artificial intelligence  
 564 and statistics*, pp. 215–223. JMLR Workshop and Conference Proceedings, 2011.

565 Thomas M Cover. *Elements of information theory*. John Wiley & Sons, 1999.

566 Jia Deng, Wei Dong, Richard Socher, Li-Jia Li, Kai Li, and Li Fei-Fei. Imagenet: A large-scale hier-  
 567 archical image database. In *2009 IEEE Conference on Computer Vision and Pattern Recognition*,  
 568 pp. 248–255, 2009. doi: 10.1109/CVPR.2009.5206848.  
 569

570 Alexey Dosovitskiy, Lucas Beyer, Alexander Kolesnikov, Dirk Weissenborn, Xiaohua Zhai, Thomas  
 571 Unterthiner, Mostafa Dehghani, Matthias Minderer, Georg Heigold, Sylvain Gelly, et al. An  
 572 image is worth 16x16 words: Transformers for image recognition at scale. *arXiv preprint  
 573 arXiv:2010.11929*, 2020.

574

575 Debidatta Dwibedi, Yusuf Aytar, Jonathan Tompson, Pierre Sermanet, and Andrew Zisserman. With  
 576 a little help from my friends: Nearest-neighbor contrastive learning of visual representations. In  
 577 *Proceedings of the IEEE/CVF International Conference on Computer Vision*, pp. 9588–9597, 2021.

578

579 Aleksandr Ermolov, Aliaksandr Siarohin, Enver Sangineto, and Nicu Sebe. Whitening for Self-  
 580 Supervised Representation Learning. In *Proceedings of the 38th International Conference on  
 581 Machine Learning*, pp. 3015–3024. PMLR, July 2021. URL <https://proceedings.mlr.press/v139/ermolov21a.html>. ISSN: 2640-3498.

582

583 Imanol G. Estepa, Ignacio Sarasua, Bhalaji Nagarajan, and Petia Radeva. All4one: Symbiotic  
 584 neighbour contrastive learning via self-attention and redundancy reduction. In *Proceedings of  
 585 the IEEE/CVF International Conference on Computer Vision (ICCV)*, pp. 16243–16253, October  
 586 2023.

587

588 Mark Everingham, Luc Van Gool, Christopher KI Williams, John Winn, and Andrew Zisserman. The  
 589 pascal visual object classes (voc) challenge. *International journal of computer vision*, 88:303–338,  
 590 2010.

591

592 Quentin Garrido, Yubei Chen, Adrien Bardes, Laurent Najman, and Yann Lecun. On the duality  
 593 between contrastive and non-contrastive self-supervised learning, October 2022. URL <http://arxiv.org/abs/2206.02574>. arXiv:2206.02574 [cs].

594 Jean-Bastien Grill, Florian Strub, Florent Altché, Corentin Tallec, Pierre H. Richemond, Elena  
 595 Buchatskaya, Carl Doersch, Bernardo Avila Pires, Zhaohan Daniel Guo, Mohammad Gheshlaghi  
 596 Azar, Bilal Piot, Koray Kavukcuoglu, Rémi Munos, and Michal Valko. Bootstrap your own latent:  
 597 A new approach to self-supervised Learning, September 2020. URL <http://arxiv.org/abs/2006.07733>. arXiv:2006.07733 [cs, stat].

598

599 Michael Gutmann and Aapo Hyvärinen. Noise-contrastive estimation: A new estimation principle  
 600 for unnormalized statistical models. In *Proceedings of the thirteenth international conference on*  
 601 *artificial intelligence and statistics*, pp. 297–304. JMLR Workshop and Conference Proceedings,  
 602 2010.

603

604 Jeff Z HaoChen, Colin Wei, Adrien Gaidon, and Tengyu Ma. Provable guarantees for self-supervised  
 605 deep learning with spectral contrastive loss. *Advances in Neural Information Processing Systems*,  
 606 34:5000–5011, 2021.

607

608 Kaiming He, Haoqi Fan, Yuxin Wu, Saining Xie, and Ross Girshick. Momentum Contrast for  
 609 Unsupervised Visual Representation Learning. Technical Report arXiv:1911.05722, arXiv, March  
 610 2020. URL <http://arxiv.org/abs/1911.05722>. arXiv:1911.05722 [cs] type: article.

611

612 Kaiming He, Xinlei Chen, Saining Xie, Yanghao Li, Piotr Dollár, and Ross Girshick. Masked  
 613 Autoencoders Are Scalable Vision Learners, December 2021. URL <http://arxiv.org/abs/2111.06377>. arXiv:2111.06377 [cs].

614

615 R Devon Hjelm, Alex Fedorov, Samuel Lavoie-Marchildon, Karan Grewal, Phil Bachman, Adam  
 616 Trischler, and Yoshua Bengio. Learning deep representations by mutual information estimation  
 617 and maximization. *arXiv preprint arXiv:1808.06670*, 2018.

618

619 Tianyang Hu, Zhili Liu, Fengwei Zhou, Wenjia Wang, and Weiran Huang. Your contrastive learning  
 620 is secretly doing stochastic neighbor embedding. *arXiv preprint arXiv:2205.14814*, 2022.

621

622 Junqiang Huang, Xiangwen Kong, and Xiangyu Zhang. Revisiting the Critical Factors of  
 623 Augmentation-Invariant Representation Learning. In Shai Avidan, Gabriel Brostow, Moustapha  
 624 Cissé, Giovanni Maria Farinella, and Tal Hassner (eds.), *Computer Vision – ECCV 2022, Lecture  
 625 Notes in Computer Science*, pp. 42–58, Cham, 2022. Springer Nature Switzerland. ISBN  
 978-3-031-19821-2. doi: 10.1007/978-3-031-19821-2\_3.

626

627 Alex Krizhevsky, Geoffrey Hinton, et al. Learning multiple layers of features from tiny images. 2009.

628

629 Phuc H Le-Khac, Graham Healy, and Alan F Smeaton. Contrastive representation learning: A  
 630 framework and review. *arXiv preprint arXiv:2010.05113*, 2020.

631

632 Jason D Lee, Qi Lei, Nikunj Saunshi, and Jiacheng Zhuo. Predicting what you already know  
 633 helps: Provable self-supervised learning. *Advances in Neural Information Processing Systems*, 34:  
 309–323, 2021.

634

635 Shuo Li, Fang Liu, Licheng Jiao, Puhua Chen, and Lingling Li. Self-Supervised Self-Organizing  
 636 Clustering Network: A Novel Unsupervised Representation Learning Method. *IEEE Transactions  
 637 on Neural Networks and Learning Systems*, pp. 1–15, 2022. ISSN 2162-2388. doi: 10.1109/  
 638 TNNLS.2022.3185638. Conference Name: IEEE Transactions on Neural Networks and Learning  
 Systems.

639

640 Shuo Li, Fang Liu, Zehua Hao, Licheng Jiao, Xu Liu, and Yuwei Guo. Minent: Minimum entropy  
 641 for self-supervised representation learning. *Pattern Recognition*, 138:109364, 2023.

642

643 Wenye Lin, Yifeng Ding, Zhixiong Cao, and Hai-Tao Zheng. Establishing a Stronger Baseline for  
 644 Lightweight Contrastive Models. In *2023 IEEE International Conference on Multimedia and Expo  
 (ICME)*, pp. 1062–1067, 2023. doi: 10.1109/ICME55011.2023.00186.

645

646 Yixin Liu, Zhao Li, Shirui Pan, Chen Gong, Chuan Zhou, and George Karypis. Anomaly detection  
 647 on attributed networks via contrastive self-supervised learning. *IEEE Transactions on Neural  
 Networks and Learning Systems*, 33(6):2378–2392, 2022. doi: 10.1109/TNNLS.2021.3068344.

648 Shentong Mo, Zhun Sun, and Chao Li. Multi-Level Contrastive Learning for Self-Supervised  
 649 Vision Transformers. pp. 2778–2787, 2023. URL [https://openaccess.thecvf.com/content/WACV2023/html/Mo\\_Multi-Level\\_Contrastive\\_Learning\\_for\\_Self-Supervised\\_Vision\\_Transformers\\_WACV\\_2023\\_paper.html](https://openaccess.thecvf.com/content/WACV2023/html/Mo_Multi-Level_Contrastive_Learning_for_Self-Supervised_Vision_Transformers_WACV_2023_paper.html).

650

651

652 Chingis Oinar, Binh M. Le, and Simon S. Woo. Expectation-Maximization via Pretext-Invariant Rep-  
 653 resentations. *IEEE Access*, 11:65266–65276, 2023. ISSN 2169-3536. doi: 10.1109/ACCESS.2023.  
 654 3289589. URL <https://ieeexplore.ieee.org/abstract/document/10163821>.  
 655 Conference Name: IEEE Access.

656

657 Aaron van den Oord, Yazhe Li, and Oriol Vinyals. Representation learning with contrastive predictive  
 658 coding. *arXiv preprint arXiv:1807.03748*, 2018.

659

660 Maxime Oquab, Timothée Darcet, Théo Moutakanni, Huy Vo, Marc Szafraniec, Vasil Khalidov,  
 661 Pierre Fernandez, Daniel Haziza, Francisco Massa, Alaeldin El-Nouby, Mahmoud Assran, Nicolas  
 662 Ballas, Wojciech Galuba, Russell Howes, Po-Yao Huang, Shang-Wen Li, Ishan Misra, Michael  
 663 Rabbat, Vasu Sharma, Gabriel Synnaeve, Hu Xu, Hervé Jegou, Julien Mairal, Patrick Labatut,  
 664 Armand Joulin, and Piotr Bojanowski. DINOv2: Learning Robust Visual Features without  
 665 Supervision, April 2023. URL <http://arxiv.org/abs/2304.07193>. arXiv:2304.07193  
 666 [cs].

667

668 Serdar Ozsoy, Shadi Hamdan, Sercan Arik, Deniz Yuret, and Alper Erdogan. Self-  
 669 Supervised Learning with an Information Maximization Criterion. *Advances in  
 670 Neural Information Processing Systems*, 35:35240–35253, December 2022. URL  
 671 [https://proceedings.neurips.cc/paper\\_files/paper/2022/hash/e4cd50120b6d7e8daff1749d6bbaa889-Abstract-Conference.html](https://proceedings.neurips.cc/paper_files/paper/2022/hash/e4cd50120b6d7e8daff1749d6bbaa889-Abstract-Conference.html).

672

673 Prajit Ramachandran, Barret Zoph, and Quoc V Le. Searching for activation functions. *arXiv preprint  
 arXiv:1710.05941*, 2017.

674

675 Shaoqing Ren, Kaiming He, Ross Girshick, and Jian Sun. Faster r-cnn: Towards real-time object  
 676 detection with region proposal networks. *IEEE transactions on pattern analysis and machine  
 677 intelligence*, 39(6):1137–1149, 2016.

678

679 Nikunj Saunshi, Orestis Plevrakis, Sanjeev Arora, Mikhail Khodak, and Hrishikesh Khandeparkar. A  
 680 theoretical analysis of contrastive unsupervised representation learning. In *International Conference on Machine Learning*, pp. 5628–5637. PMLR, 2019.

681

682 Kendrick Shen, Robbie M Jones, Ananya Kumar, Sang Michael Xie, Jeff Z HaoChen, Tengyu Ma,  
 683 and Percy Liang. Connect, not collapse: Explaining contrastive learning for unsupervised domain  
 684 adaptation. In *International conference on machine learning*, pp. 19847–19878. PMLR, 2022.

685

686 Zhiqian Tan, Yifan Zhang, Jingqin Yang, and Yang Yuan. Contrastive learning is spectral clustering  
 687 on similarity graph. *arXiv preprint arXiv:2303.15103*, 2023.

688

689 Yonglong Tian, Dilip Krishnan, and Phillip Isola. Contrastive Multiview Coding. In Andrea Vedaldi,  
 690 Horst Bischof, Thomas Brox, and Jan-Michael Frahm (eds.), *Computer Vision – ECCV 2020*,  
 691 Lecture Notes in Computer Science, pp. 776–794, Cham, 2020a. Springer International Publishing.  
 ISBN 978-3-030-58621-8. doi: 10.1007/978-3-030-58621-8\_45.

692

693 Yonglong Tian, Chen Sun, Ben Poole, Dilip Krishnan, Cordelia Schmid, and Phillip  
 694 Isola. What Makes for Good Views for Contrastive Learning? In *Advances  
 695 in Neural Information Processing Systems*, volume 33, pp. 6827–6839. Curran  
 696 Associates, Inc., 2020b. URL <https://proceedings.neurips.cc/paper/2020/hash/4c2e5eaae9152079b9e95845750bb9ab-Abstract.html>.

697

698 Yuandong Tian. Deep contrastive learning is provably (almost) principal component analysis. *arXiv  
 699 preprint arXiv:2201.12680*, 3, 2022.

700

701 Shengbang Tong, Yubei Chen, Yi Ma, and Yann Lecun. EMP-SSL: Towards Self-Supervised  
 702 Learning in One Training Epoch, April 2023. URL <http://arxiv.org/abs/2304.03977>.  
 arXiv:2304.03977 [cs].

702 Shirui Wang, Wenyi Hu, Pengyu Yuan, Xuqing Wu, Qunshan Zhang, Prashanth Nadukandi, Ger-  
 703 man Ocampo Botero, and Jiefu Chen. A self-supervised deep learning method for seismic data  
 704 deblending using a blind-trace network. *IEEE Transactions on Neural Networks and Learning*  
 705 *Systems*, 34(7):3405–3414, 2023. doi: 10.1109/TNNLS.2022.3188915.

706 Tongzhou Wang and Phillip Isola. Understanding contrastive representation learning through align-  
 707 ment and uniformity on the hypersphere. In *International conference on machine learning*, pp.  
 708 9929–9939. PMLR, 2020.

709 Yifei Wang, Qi Zhang, Yisen Wang, Jiansheng Yang, and Zhouchen Lin. Chaos is a ladder: A  
 710 new theoretical understanding of contrastive learning via augmentation overlap. *arXiv preprint*  
 711 *arXiv:2203.13457*, 2022.

712 Chen Wei, Haoqi Fan, Saining Xie, Chao-Yuan Wu, Alan Yuille, and Christoph Feichtenhofer.  
 713 Masked Feature Prediction for Self-Supervised Visual Pre-Training. pp. 14668–14678, 2022. URL  
 714 [https://openaccess.thecvf.com/content/CVPR2022/html/Wei\\_Masked\\_Feature\\_Prediction\\_for\\_Self-Supervised\\_Visual\\_Pre-Training\\_CVPR\\_2022\\_paper.html](https://openaccess.thecvf.com/content/CVPR2022/html/Wei_Masked_Feature_Prediction_for_Self-Supervised_Visual_Pre-Training_CVPR_2022_paper.html).

715 Zhirong Wu, Zihang Lai, Xiao Sun, and Stephen Lin. Extreme Masking for Learning Instance  
 716 and Distributed Visual Representations, March 2023. URL <http://arxiv.org/abs/2206.04667> [cs].

717

718 Zhenda Xie, Zheng Zhang, Yue Cao, Yutong Lin, Jianmin Bao, Zhuliang Yao, Qi Dai, and Han Hu.  
 719 SimMIM: A Simple Framework for Masked Image Modeling. pp. 9653–9663, 2022. URL [https://openaccess.thecvf.com/content/CVPR2022/html/Xie\\_SimMIM\\_A\\_Simple\\_Framework\\_for\\_Masked\\_Image\\_Modeling\\_CVPR\\_2022\\_paper.html](https://openaccess.thecvf.com/content/CVPR2022/html/Xie_SimMIM_A_Simple_Framework_for_Masked_Image_Modeling_CVPR_2022_paper.html).

720

721 Zhengeng Yang, Hongshan Yu, Yong He, Wei Sun, Zhi-Hong Mao, and Ajmal Mian. Fully convo-  
 722 lutional network-based self-supervised learning for semantic segmentation. *IEEE Transactions*  
 723 *on Neural Networks and Learning Systems*, 35(1):132–142, 2024. doi: 10.1109/TNNLS.2022.  
 724 3172423.

725

726 Jure Zbontar, Li Jing, Ishan Misra, Yann LeCun, and Stephane Deny. Barlow Twins: Self-Supervised  
 727 Learning via Redundancy Reduction. In *Proceedings of the 38th International Conference on*  
 728 *Machine Learning*, pp. 12310–12320. PMLR, July 2021. URL <https://proceedings.mlr.press/v139/zbontar21a.html>. ISSN: 2640-3498.

729

730 Yifan Zhang, Zhiqian Tan, Jingqin Yang, Weiran Huang, and Yang Yuan. Matrix information theory  
 731 for self-supervised learning. *arXiv preprint arXiv:2305.17326*, 2023.

732

733 Jinghao Zhou, Chen Wei, Huiyu Wang, Wei Shen, Cihang Xie, Alan Yuille, and Tao Kong. iBOT:  
 734 Image BERT Pre-Training with Online Tokenizer, January 2022a. URL <http://arxiv.org/abs/2111.07832> [cs].

735

736

737 Qiang Zhou, Chaohui Yu, Hao Luo, Zhibin Wang, and Hao Li. MimCo: Masked Image Modeling  
 738 Pre-training with Contrastive Teacher. In *Proceedings of the 30th ACM International Conference*  
 739 *on Multimedia*, MM '22, pp. 4487–4495, New York, NY, USA, October 2022b. Association  
 740 for Computing Machinery. ISBN 978-1-4503-9203-7. doi: 10.1145/3503161.3548173. URL  
 741 <https://doi.org/10.1145/3503161.3548173>.

742

743 Roland S Zimmermann, Yash Sharma, Steffen Schneider, Matthias Bethge, and Wieland Brendel.  
 744 Contrastive learning inverts the data generating process. In *International Conference on Machine*  
 745 *Learning*, pp. 12979–12990. PMLR, 2021.

746

747

748

749

750

751

752

753

754

755

756 SUPPLEMENTARY MATERIALS  
757758 A THE USE OF LARGE LANGUAGE MODELS (LLMs)  
759760 In preparing this manuscript, we employed large language models (LLMs) solely for language  
761 polishing and grammar refinement. The LLMs were not involved in idea generation, theoretical  
762 development, algorithm design, experimental implementation, or result analysis. All technical content,  
763 experiments, and conclusions presented in this work are entirely the contribution of the authors.  
764765 B THEORETICAL JUSTIFICATION FOR THE IE-CL FRAMEWORK  
766767 This appendix provides a detailed theoretical argument for our proposed Incremental Entropy Con-  
768 trastive Learning (IE-CL) framework. We first establish why maximizing the entropy of negative  
769 sample representations,  $H(Z'^-)$ , is a desirable objective within the InfoNCE framework. We then  
770 use the Data-Processing Inequality to formally demonstrate why naively maximizing input-level  
771 entropy is insufficient due to the information bottleneck of deep encoders. Finally, we show how our  
772 full IE-CL objective function provides a principled and complete solution to this challenge.  
773774 B.1 THE GOAL: MAXIMIZING NEGATIVE ENTROPY FOR BETTER CONTRASTIVE LEARNING  
775776 The standard InfoNCE loss for a positive pair  $(z, z^+)$  and a set of  $N - 1$  negative samples  $\{z_k^-\}_{k=1}^{N-1}$   
777 drawn from a distribution  $q(z^-)$  is:  
778

779 
$$\mathcal{L}_{\text{InfoNCE}} = -\mathbb{E} \left[ \log \frac{\exp(s(z, z^+)/\tau)}{\exp(s(z, z^+)/\tau) + (N-1)\mathbb{E}_{z^- \sim q}[\exp(s(z, z^-)/\tau)]} \right] \quad (18)$$
  
780

781 Our core premise is that increasing the entropy of the negative distribution,  $H(Z'^-)$ , where  $q$  is the  
782 distribution of  $Z'^-$ , makes the contrastive task more challenging and thus compels the model to learn  
783 better representations. Let's formalize this.  
784785 The denominator of the InfoNCE loss can be seen as a partition function. A higher entropy  $H(Z'^-)$   
786 implies that the negative samples  $z^-$  are more diverse and spread out in the representation space.  
787 This increased diversity makes it statistically more likely for some negative samples to be close to the  
788 anchor  $z$ , thus increasing the expected value of the negative scores,  $\mathbb{E}_{z^- \sim q}[\exp(s(z, z^-)/\tau)]$ .  
789790 This directly increases the value of the denominator, which in turn increases the InfoNCE loss. To  
791 compensate for this more difficult learning signal (i.e., to minimize the loss), the optimizer is forced  
792 to adapt the encoder parameters  $(\theta_1, \theta_2)$  to create a sharper separation. This is primarily achieved by  
793 increasing the similarity of the positive pair,  $s(z, z^+) \uparrow$ .  
794795 An increased positive pair similarity implies that given an anchor  $z$ , its positive counterpart  $z^+$   
796 becomes more predictable. In information-theoretic terms, this corresponds to a reduction in the  
797 conditional entropy,  $H(Z^+|Z) \downarrow$ . According to the definition of mutual information,  $I(Z; Z^+) =$   
798  $H(Z^+) - H(Z^+|Z)$ , a decrease in conditional entropy (while the marginal entropy  $H(Z^+)$  is kept  
799 non-trivial to prevent collapse) leads to an increase in the mutual information,  $I(Z; Z^+) \uparrow$ . This is  
800 the ultimate goal of InfoNCE-based contrastive learning.  
801802 Thus, we have established the following desirable causal relationship:  
803

804 
$$\max H(Z'^-) \implies \min H(Z^+|Z) \implies \max I(Z; Z^+) \iff \min \mathcal{L}_{\text{InfoNCE}} \quad (19)$$
  
805

806 This confirms that maximizing the entropy of negative representations is a valid and principled  
807 objective for improving contrastive representation learning.  
808

## 809 B.2 THE CHALLENGE: THE INFORMATION BOTTLENECK IN DEEP ENCODERS

810 Having established our goal, the naive strategy would be to simply maximize the entropy at the input  
811 of the encoder,  $H(X'^-)$ , using our SAIB module,  $g_\phi$ . However, this approach is fundamentally  
812 flawed because it ignores the transformative effect of the deep encoder,  $f_\theta$ .  
813

810 The Data-Processing Inequality for differential entropy provides a formal tool to analyze this. Let  
 811  $X'^- = g_\phi(X^-)$  be the transformed input. The entropy of the final representation,  $Z'^- = f_\theta(X'^-)$ ,  
 812 is bounded by the entropy of its input  $H(X'^-)$ :

$$813 \quad H(Z'^-) = H(f_\theta(X'^-)) \leq H(X'^-) + \mathbb{E}_{p(x')}[\log |\det J_{f_\theta}(x')|] \quad (20)$$

814 where  $J_{f_\theta}(x')$  is the Jacobian of the encoder function  $f_\theta$  evaluated at  $x'$ .

815 This inequality reveals the core challenge. While our SAIB module is designed to maximize  $H(X'^-)$ ,  
 816 the second term,  $\mathbb{E}[\log |\det J_{f_\theta}|]$ , which depends entirely on the encoder, can be a large negative  
 817 value. This occurs if the encoder acts as a severe **information bottleneck**, aggressively compressing  
 818 or collapsing its input space. In such a scenario, the entropy gained at the input level via SAIB would  
 819 be nullified by the entropy lost during the encoding process.

820 Therefore, we conclude that maximizing the input-level incremental entropy  $\Delta H(X^-)$  (and thus  
 821  $H(X'^-)$ ) is a **necessary but not sufficient** condition. To robustly increase the final representation  
 822 entropy  $H(Z'^-)$ , a mechanism to control the encoder’s information-compressing behavior is essential.

### 823 B.3 THE IE-CL SOLUTION: A SYNERGISTIC OPTIMIZATION FRAMEWORK

824 Our IE-CL framework provides a complete solution by reformulating the objective to jointly optimize  
 825 both entropy generation and preservation. We re-state our final loss function from the main text:

$$826 \quad \mathcal{L}_{\text{final}} = \mathcal{L}_{\text{InfoNCE}} + \beta D_{\text{KL}}(p_\phi || q) - \lambda H(Z'^-) + \eta \mathcal{L}_{\text{reg\_encoder}} \quad (21)$$

827 Let’s analyze how this objective creates an optimization landscape that solves the challenge described  
 828 in Sec. B.2. The goal of the optimizer is to minimize  $\mathcal{L}_{\text{final}}$ , which is dominated by the term  
 829  $-\lambda H(Z'^-)$ , effectively becoming an objective to maximize  $H(Z'^-)$ . To achieve this, the optimizer  
 830 can adjust the parameters of SAIB ( $\phi$ ) and the encoder ( $\theta$ ).

- 831 **1. Optimizing SAIB ( $\phi$ ):** To maximize the final entropy  $H(Z'^-)$ , the optimizer is incentivized  
 832 to maximize the input entropy  $H(X'^-)$ , as established by the bound in Eq. 20. The SAIB  
 833 module,  $g_\phi$ , is specifically designed for this task. As shown in the appendix, its design as a  
 834 volume-expanding map ( $|\det J_{g_\phi}| > 1$ ) directly translates to maximizing the incremental  
 835 entropy  $\Delta H(X^-)$ . This is the **entropy generation** part of our framework.
- 836 **2. Optimizing the Encoder ( $\theta$ ):** The term  $\eta \mathcal{L}_{\text{reg\_encoder}}$  directly constrains the encoder. By  
 837 implementing this regularizer via **Spectral Normalization**, we constrain the Lipschitz  
 838 constant of the encoder’s layers. A smaller Lipschitz constant leads to a "smoother"  
 839 transformation, which in turn prevents the Jacobian determinant term  $\mathbb{E}[\log |\det J_{f_\theta}|]$  from  
 840 becoming excessively negative. This term directly counteracts the information bottleneck,  
 841 serving as the **entropy preservation** part of our framework.
- 842 **3. Semantic Constraint ( $D_{KL}$ ):** The KL-divergence term acts as a crucial regularizer on SAIB,  
 843 ensuring that the entropy maximization process does not push the transformed samples  $X'^-$   
 844 into a semantically meaningless or out-of-distribution space.

845 In conclusion, the IE-CL objective function does not assume a naive carry-over of entropy. Instead,  
 846 it creates a synergistic system where the only effective way for the optimizer to maximize the final  
 847 representation entropy  $H(Z'^-)$  is to **simultaneously** use SAIB to generate rich input entropy and  
 848 constrain the encoder to faithfully preserve it. This provides a principled and robust solution to  
 849 learning diverse representations for contrastive learning.

## 850 C JACOBIAN DETERMINANT OF THE SAIB

### 851 C.1 DETAILS OF THE SAIB

852 **Block definition.** Let  $x \in \mathbb{R}^D$  be the flattened patchified tensor. Within a fixed ReLU activation  
 853 pattern the block acts linearly:

$$854 \quad f(x) = x + A x, \quad A := W_4 M_3 W_3 M_2 W_2 M_1 W_1, \quad (22)$$

855 where

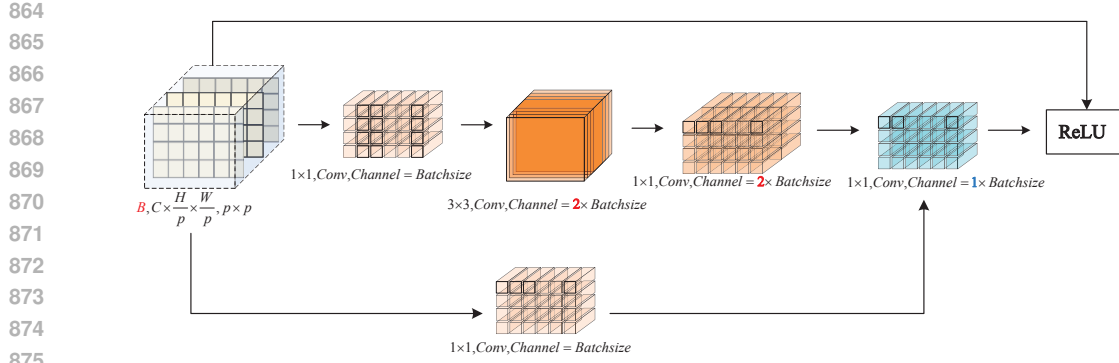


Figure 6: Structure of Sample Augmentation Incremental Block (**SAIB**). Note that due to the patching of the 3-channel image, the batch occupies the position of the original channel. Therefore, it is possible to drive the inter-batch information to communicate by changing the original convolutional channels. All the convolutions in this block are cascaded with BN layers and SwishRamachandran et al. (2017) to achieve nonlinear augmentation capability. And then convolved and non-linearly processed, and finally reconstructed back to the original position through positional coding.

- $W_1 \in \mathbb{R}^{D \times D}$ ,  $W_3 \in \mathbb{R}^{2D \times 2D}$ ,  $W_4 \in \mathbb{R}^{D \times 2D}$  are  $1 \times 1$ -convs;
- $W_2 \in \mathbb{R}^{2D \times D}$  is a  $3 \times 3$ -conv that *doubles* the channel dimension;
- $M_i$  are diagonal 0/1 masks coming from ReLU derivatives.

**Step 1: A lower bound on  $\|A\|_2$ .** Because  $W_2$  maps  $\mathbb{R}^D \rightarrow \mathbb{R}^{2D}$  with i.i.d. Gaussian initialisation of variance  $2/\text{fan}_{\text{in}}$ , random matrix theory gives

$$\Pr[\sigma_{\max}(W_2) \geq \sqrt{2}] = 1. \quad (23)$$

All other  $W_i$  are square and full rank by construction, so  $\|A\|_2 \geq \sqrt{2} \|W_4 M_3 W_3 M_1 W_1\|_2 > 1$  almost surely.

**Step 2: Singular values of the Jacobian.** The Jacobian of  $f$  is

$$J = I + A. \quad (24)$$

Let  $u$  be the right singular vector of  $A$  associated with  $\sigma_{\max}(A) =: s > 1$ . Then

$$\|Ju\|_2 = \|u + Au\|_2 \geq \|Au\|_2 - \|u\|_2 = s - 1 > 0, \quad (25)$$

and by triangle inequality also  $\|Ju\|_2 \geq 1 + s$ . Hence the largest singular value of  $J$  satisfies  $\sigma_{\max}(J) \geq 1 + s > 2$ .

**Step 3: Determinant strictly greater than 1.** Since  $J$  is the sum of identity and a matrix of full column rank, every singular value of  $J$  is  $\geq 1$  (see Weyl's monotonicity theorem). With at least one singular value  $> 2$  we get

$$|\det J| = \prod_{k=1}^D \sigma_k(J) > 2 \times 1^{D-1} > 1. \quad (26)$$

Therefore the block is *locally volume-expanding* almost everywhere, and its differential entropy change  $\Delta H = \mathbb{E}[\log |\det J|] > 0$ .

**Remark.** Even if some ReLU masks set entire channels to zero, the  $2 \times$  expansion ensures that at least one singular value of  $A$  remains  $> 1$  with high probability, keeping the argument intact.

918 D TRAINING COST  
919  
920  
921  
922  
923

924 We show a comparison of the training time consumed for the proposed strategies in Figure 7 and  
925 Figure 8, respectively. Figure 7 shows the different methods at 256 batch setting a with resnet50  
926 as backbone on ImageNet-1k. The time required to train one epoch. All parameters were kept at  
927 the optimal settings declared at the time of their release, and time spent was evaluated using mixed  
928 precision on 8×V100 (32G).

929 Figure 8 illustrates the additional computational time consumption associated with the SAIB plug-  
930 and-play existing approach. Due to the differences in the self-supervised paradigms, we observe that  
931 for the encoder half-update paradigm (MoCo-v2, SimSiam, BYOL), adding SAIB to maximise the  
932 incremental information entropy results in only a slight additional computation time (within 10%),  
933 whereas for the full-parameter update approach that relies heavily on the batch scaling to function  
934 (SimCLR), adding SAIB increases the training time by 12.3%. Overall, SAIB is able to balance the  
935 performance improvement of the model with the increased training time.

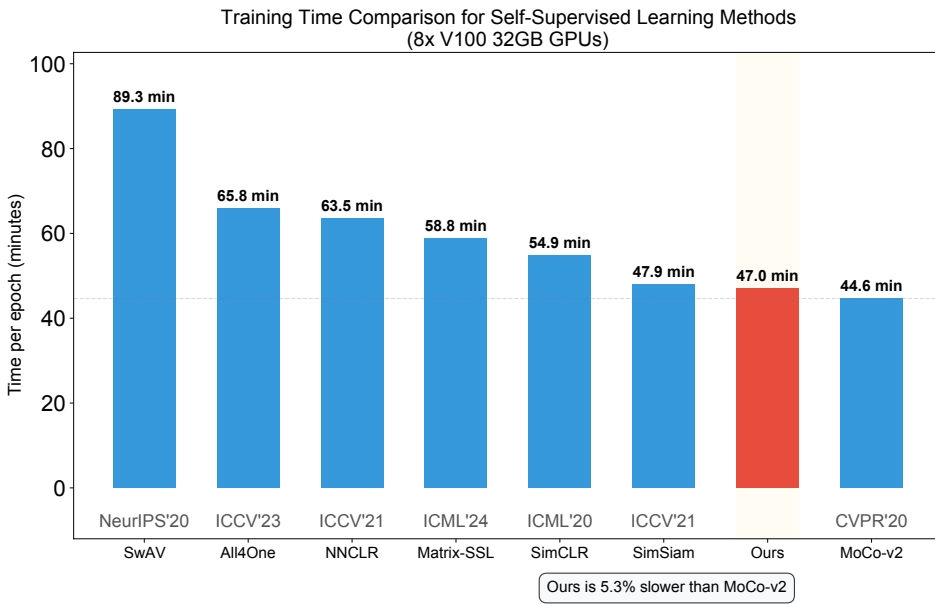


Figure 7: Comparison of the time taken by different methods to train an epoch on ImageNet-1k with batch of 256. The proposed IE-CL, although it includes an additional non-isometric transform module SAIB, still spends less training cost compared to the previous methods because it uses momentum to update the Query encoder.

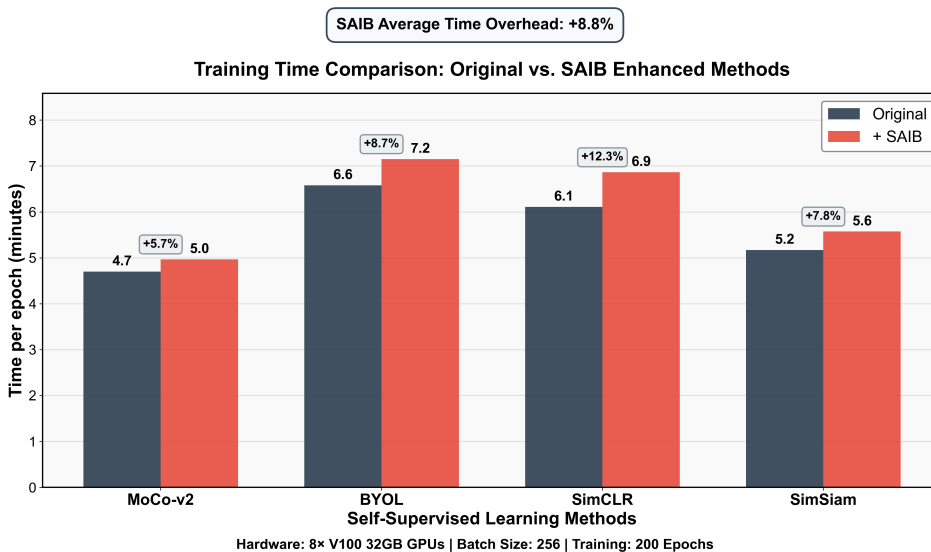


Figure 8: As a plug-and-play module, SAIB enhances the performance of existing contrastive learning methods with limited additional computational overhead. Overall, it achieves effective performance gains within an acceptable increase in training time—on average, approximately 8.8% more—compared to the original models (see Table 5 in the main text).

1026 E PSEUDO CODE  
1027

---

1028 **Algorithm 1:** PyTorch pseudo-code of IE-CL (Corrected)

---

```

1029 # Q: anchor encoder (updated by backprop)
1030 # K: query encoder (updated by momentum)
1031 # m: momentum hyperparameter for K
1032 # ctr: contrastive loss function (e.g., InfoNCE)
1033 # SAIB: sample augmentation incremental block
1034 # optimizer: updates Q and SAIB parameters
1035 # H: entropy estimator
1036 # Initialize K's parameters from Q's
1037 K.load_state_dict(Q.state_dict())
1038 for x in loader:
1039     # Create two augmented views
1040     x_anchor, x_query = aug(x), aug(x)
1041     # Apply SAIB to the query view to increase entropy
1042     x_query_transformed = SAIB(x_query)
1043     # -- Forward Pass --
1044     # Q computes features for anchor and transformed query
1045     q_anchor = Q(x_anchor)
1046     q_query_transformed = Q(x_query_transformed)
1047     # K computes features for transformed query (no gradients)
1048     with torch.no_grad():
1049         k_query = K(x_query_transformed)
1050     # -- Loss Calculation (matches Equation 25) --
1051     # 1. InfoNCE Loss
1052     L_InfoNCE = ctr(q_anchor, k_query)
1053     # 2. KL divergence for regularization
1054     L_KL = KL_Loss(q_query_transformed.detach(), q_anchor)
1055     # 3. Incremental Entropy Maximization
1056     L_entropy_max = -H(q_query_transformed)
1057     # Total loss
1058     loss = L_InfoNCE + β * L_KL + λ * L_entropy_max
1059     # -- Backward Pass & Optimizer Step --
1060     loss.backward()
1061     optimizer.step()
1062     optimizer.zero_grad()
1063     # -- Momentum Update K --
1064     with torch.no_grad():
1065         for param_q, param_k in zip(Q.parameters(), K.parameters()):
1066             param_k.data = param_k.data * m + param_q.data * (1.0 - m)
1067
1068
1069
1070
1071
1072
1073
1074
1075
1076
1077
1078
1079
```

---